Study of PET/PP/TiO_2 Microfibrillar-Structured Composites, Part 2: Morphology and Mechanical Properties

Wenjing Li,[1] Alois K. Schlarb,[1] Michael Evstatiev[2]

[1]*Institut für Verbundwerkstoffe (Institute for Composite Materials), University of Kaiserslautern, Erwin Schrödinger Str., Kaiserslautern 67663, Germany*
[2]*Laboratory on Polymers, Sofia University, Sofia 1126, Bulgaria*

Received 28 September 2008; accepted 18 February 2009
DOI 10.1002/app.30290
Published online 7 May 2009 in Wiley InterScience (www.interscience.wiley.com).

ABSTRACT: Uncompatibilized and compatibilized (polypropylene grafted maleic anhydride as compatibilizer) polyethylene terephthalate (PET)/polypropylene (PP)/TiO_2 microfibrillar composites (MFC) were prepared by injection molding of the pelletized PET/PP/TiO_2 drawn strands. The morphology of PET fibrils and the distribution of TiO_2 particles in the composites were examined. After injection molding the preferential location of TiO_2 particles is still preserved. Because of the reinforcement effect of PET fibrils, the tensile properties and impact strength of the PET/PP MFC are improved compared with the pure PP. Incorporation of TiO_2 particles results in decrease of both tensile strength and impact strength of the composites. However, the compatibilized PET/PP/TiO_2 MFC demonstrate better mechanical properties compared with the uncompatibilized ones. DMA analysis shows that the glass transition temperature (T_g) of PET in the uncompatibilized PET/PP/TiO_2 MFC and the T_g of PP in the compatibilized PET/PP/TiO_2 MFC are elevated by about 2°C. The elevation of T_g is attributed to the preferential location of TiO_2 particles in the composites. © 2009 Wiley Periodicals, Inc. J Appl Polym Sci 113: 3300–3306, 2009

Key words: nanocomposites; reinforcement; fibrils; impact strength; DMA

INTRODUCTION

Ternary nanocomposites of polymer blends and nanofillers have been widely investigated because it is found that the nanofillers affect the phase behavior and lead to a compatibilization effect on the polymer blends.[1–3] Generally, in polymer blends, the nanoparticles are either dispersed in one phase or located at the interface depending on the interfacial tension between the polymer and nanoparticles, the viscosity of the polymers and the kinetic factor (e.g., blending sequence)[4–7]. In addition to studying the phase morphology, the effects of nanofillers on the thermal and mechanical properties of ternary nanocomposites have been also investigated.[8,9] As expected, the incorporated nanofillers generally impart their high stiffness to the blends. However, material strength that is strongly dependent on interfacial adhesion was reported to be moderately increased[7,10,11] or slightly decreased.[12]

Polyethylene terephthalate (PET) and polypropylene (PP) are known to be fully immiscible and require interfacial modification to obtain good emulsification and to increase the solid-state adhesion. Numerous investigations have been performed to compatibilize PET and PP with different types of compatibilizer containing maleic anhydride (MA), acrylic acid, or glycidyl methacrylate functionality.[13–17] The incorporated compatibilizer decreases the interfacial tension between PET and PP, thus leading to a finer morphology of the blends.[18] The mechanical properties of compatibilized PET/PP blends were also reported to be improved.[19,20]

Microfibrillar composites (MFC) that are reinforced by *in situ* formed polymer fibrils exhibit improved mechanical properties compared with the matrix polymer,[21–24] as the polymer fibrils act as reinforcement for the polymer matrix. The incorporation of inorganic filler into microfibrillar-structured composites may further influence the mechanical properties of the composites. In the previous experiment, two types of TiO_2 particles (300 nm and 15 nm in diameter) were incorporated into both uncompatibilized and compatibilized PET/PP blend (PP-*g*-MA as compatibilizer), PET/PP/TiO_2 drawn strands were prepared by stretching the extrudates. It was found that in the uncompatibilized drawn strands, both types of TiO_2 particles are exclusively

Correspondence to: W. Li (wenjing.li@ivw.uni-kl.de).
Contract grant sponsors: BASF (the chemical company), DFG (German Science Foundation) (Graduate school GK 814).

TABLE I
Material Designation and Composition of PET/PP/TiO_2 MFC

Designation	Composition	Parts (volume ratio)
PET/PP	PET/PP	25/75
PET/PP/C	PET/PP/PP-*g*-MA	25/72/3
PET/PP/2T300	PET/PP/TiO_2-300 nm	24.5/73.5/2
PET/PP/C/2T300	PET/PP/PP-*g*-MA/TiO_2-300 nm	24.5/70.5/3/2
PET/PP/4T300	PET/PP/TiO_2-300 nm	24/72/4
PET/PP/C/4T300	PET/PP/PP-*g*-MA/TiO_2-300 nm	24/69/3/4
PET/PP/2T15	PET/PP/TiO_2-15 nm	24.5/73.5/2
PET/PP/C/2T15	PET/PP/PP-*g*-MA/TiO_2-15 nm	24.5/70.5/3/2

dispersed in the PET fibrils; whereas in the compatibilized drawn strands (with 3 vol % of compatibilizer), the TiO_2-300-nm particles are preferentially distributed in the PP phase, the TiO_2-15-nm particles are dispersed in both PET fibrils and PP phase. This preferential location of TiO_2 particles results in different structures of the PET/PP/TiO_2 drawn strands, which brings forth different but interesting dynamic mechanical behaviors of the drawn strands.[25]

In this study, PET/PP/TiO_2 MFC were prepared by injection molding of the pelletized PET/PP/TiO_2 drawn strands. The purpose of this study is to investigate the effect of the preferential location of TiO_2 particles on the static and dynamic mechanical properties of the MFC.

EXPERIMENTAL

Materials and sample preparation

PET was provided by SK Chemicals (skyPET BL8050) with the intrinsic viscosity of 0.80 dL/g, PP was purchased from Basell (Novolen). PP-*g*-MA supplied by ATOfina (OREVAC CA 100) was used as compatibilizer for PET and PP. Two types of TiO_2 particles (Kronos 2220 and RM300) were supplied by Kronos and Sachtleben Chemie GmbH, respectively. The mean diameters of the two types of particles were 300 nm for Kronos 2220 and 15 nm for RM300, respectively. Both types were used as received.

Pure PET was dried for 12 h at 100°C to avoid its hydrolytic degradation during extrusion. PP-*g*-MA was dried for 12 h at 80°C. PP was firstly extruded with 4 vol % (and 7 vol %) of TiO_2 (both Kronos 2220 and RM300) in a Berstorff twin-screw extruder using an optimized extrusion technique. The obtained PP/TiO_2 nanocomposite was then premixed with PET in presence (or absence) of PP-*g*-MA. The premixed materials were extruded in a Brabender twin-screw extruder under the screw speed of 40 rpm. The temperature zones from hopper to die were set at 230, 270, 275, 275°C.

After coming out of the extruder (2 mm capillary die), the extrudate was immediately cooled down to 85°C and drawn by a stretching device as it is described before.[26–28] The draw ratio that is defined as the ratio between the crosssection areas of the drawn strand and the die was always kept at 10. The drawn strands were then pelletized into small pieces (3 mm in length) and injection molded into dog-bone specimens by an injection molding machine (Arburg 320S). The temperatures of different zones were (from the hopper to the die): 175, 190, 190, 195, 200°C. The screw speed was 450 rpm and the injection pressure was kept at around 60 MPa. For comparison purpose, PET/PP MFC and PP were also prepared by injection molding. To subject the pure PP to the same thermal mechanical history as that of the PP in the PET/PP/TiO_2 MFC, the PP was extruded twice before injection molding. The designation and composition of the PET/PP/TiO_2 and PET/PP MFC are given in Table I.

Characterization

The impact-fractured surfaces of the injection-molded MFC specimens and the etched MFC (with hot xylene for 12 h) specimens were examined by scanning electron microscopes (JEOL JSM-6300 and ZEISS Supra^{TM} 40VP). All the specimens were sputtered with Pd/Pt alloy before observation.

The static tensile test of the MFC specimens were performed on a Zwick 1474 universal testing machine according to the DIN EN ISO 527. The crosshead speed was 5 mm/min. The tensile modulus was measured by an extensometer. All the data presented correspond to the average of five measurements. The Charpy impact strength of the unnotched specimens ($4 \times 10 \times 80$ mm^3) was tested according to the DIN EN ISO 179. For each material, seven specimens were tested.

Dynamic mechanical analysis of MFC was performed using a Gabo EPLEXOR 100 N dynamic mechanical analyzer with a tensile mode. The samples were measured from −30°C to 150°C at a frequency of 10 Hz with a heating rate of 2°C/min. The storage modulus and tan δ were recorded as a function of temperature.

RESULTS AND DISCUSSION

Morphology of PET fibrils

Figure 1 shows the morphology of PET fibrils in the MFC specimens after extraction of the PP matrix. It is seen from Figure 1(c–f) that the PET fibrils are much shorter and thicker compared with the fibrils in drawn strands [Figure 1(a,b)], some fibrils almost retract back to spherical shape. During injection molding of the pelletized drawn strands, the processing temperature was set at 200°C, which is high above the T_g of PET. On the one hand, the PET fibrils tend to retract due to the high temperature; on the other hand, the coalescence of PET fibrils could occur to some extent.[29] In addition, setting the screw speed at 450 rpm, the extensive shear stress inside the barrel may also break the fibrils. Consequently, the PET fibrils in the MFC demonstrate a larger diameter and a much lower aspect ratio.

It is already known from our previous study that in the uncompatibilized PET/PP/TiO_2 drawn strands, the TiO_2 particles (both TiO_2-300 nm and TiO_2-15 nm) are dispersed in the PET fibrils; whereas in the compatibilized drawn strands, the TiO_2-300 nm particles are preferentially dispersed in the PP phase, the TiO_2-15 nm particles are located in both PET fibrils and PP phase.[25] After injection molding, the preferential location of TiO_2 is still preserved as shown in Figure 1. In the uncompatibilized PET/PP/TiO_2 MFC, the TiO_2-300 nm particles are found in the curving PET fibrils [Fig. 1(c)]; whereas in the compatibilized MFC, the PET fibrils are quite clean, the TiO_2-300 nm particles are located on the surface of PET fibrils [Fig. 1(d)]. High-magnification SEM image [Fig. 1(g)] shows that in the PET/PP/2T15 MFC the PET fibrils contains lots of TiO_2-15 nm. In the PET/PP/C/2T MFC, small agglomerates of TiO_2-15 nm particles are noticed on the surface of PET fibrils [Fig. 1(h)]. These agglomerates TiO_2-15 nm particles are believed to be from the PP matrix and left on the PET fibrils after extraction of PP.

Tensile properties of PET/PP/TiO_2 MFC

Tensile properties and impact strength of the injection-molded PET/PP/TiO_2 and PET/PP MFC are given in Table II. The tensile strength of PET/PP MFC is slightly higher than that of the pure PP. Incorporation of TiO_2 particles results in a decrease in the tensile strength of MFC. The PET fibrils are expected to be the reinforcement in the MFC. However, the experimental result indicates that the reinforcement effect of PET fibrils is not considerable, which can be explained from the following three aspects. Firstly, in the injection-molded MFC specimens the PET fibrils lose their orientation and randomly distribute in the PP matrix. Secondly, the low-injection molding temperature) (200°C) results in poor interfacial adhesion between PET fibrils and PP matrix. Thirdly, as shown in Figure 1(c–f), the PET fibrils become much shorter and thicker after injection molding, resulting in a less effective reinforcement effect.

It is interesting to notice that the compatibilized PET/PP/TiO_2 MFC usually exhibit higher tensile strength compared with the uncompatibilized PET/PP/TiO_2 MFC. As seen in Figure 2(a), which shows the fracture surface of PET/PP/2T300 MFC, the preserved PET fibrils are damaged by the TiO_2-300 nm particles; whereas in the PET/PP/C/2T300 MFC, the PET fibrils are well preserved [Fig. 2(b)]. Therefore in the PET/PP/2T300 MFC, the reinforcement effect of the PET/TiO_2-300 nm fibrils becomes less effective in comparison with the PET fibrils in the PET/PP/C/2T300 MFC. In addition, for the PET/PP/C/2T300 MFC, by incorporating compatibilizer the interfacial adhesion between the PET fibrils and PP matrix is improved, which also promotes the stress transfer and leads to an increase in tensile strength.[13]

The tensile modulus of PET/PP and PET/PP/TiO_2 MFC is dramatically improved compared with the pure PP. The PET fibrils which are much stiffer and tougher than the PP contribute to this elevation of modulus.[30] The incorporation of TiO_2 particles further increases the modulus of MFC irrespective of their preferential location. Comparison among the PET/PP/TiO_2 MFC with different TiO_2 loadings (2 vol % and 4 vol %) shows that the tensile properties of PET/PP/TiO_2 MFC are not much influenced by the concentration of the TiO_2 particles.

Impact strength of PET/PP/TiO_2 MFC

The impact strength of PET/PP MFC is higher than that of the pure PP. Li et al.[31] also observed an increase in the essential work of fracture of PET/PE MFC compared with pure PE. However, other researchers reported that the impact strength of PET/PP MFC is lower than pure PP, which is opposite to our finding.[29,32] Note that in this study, the pure PP was subjected to two times extrusion before injection molding, which may deteriorate the mechanical properties of PP. In the PET/PP MFC, the tough PET fibrils contribute to the elevation of impact strength despite of the poor interfacial adhesion between the PET fibrils and PP.

The addition of TiO_2 particles decreases the impact strength of the MFC, the impact strength decreases more with increasing loading of TiO_2. Similar findings were also reported by other researchers who incorporated nanofillers into polymer blends.[8,6,33] In the PET/PP/TiO_2 MFC, irrespective

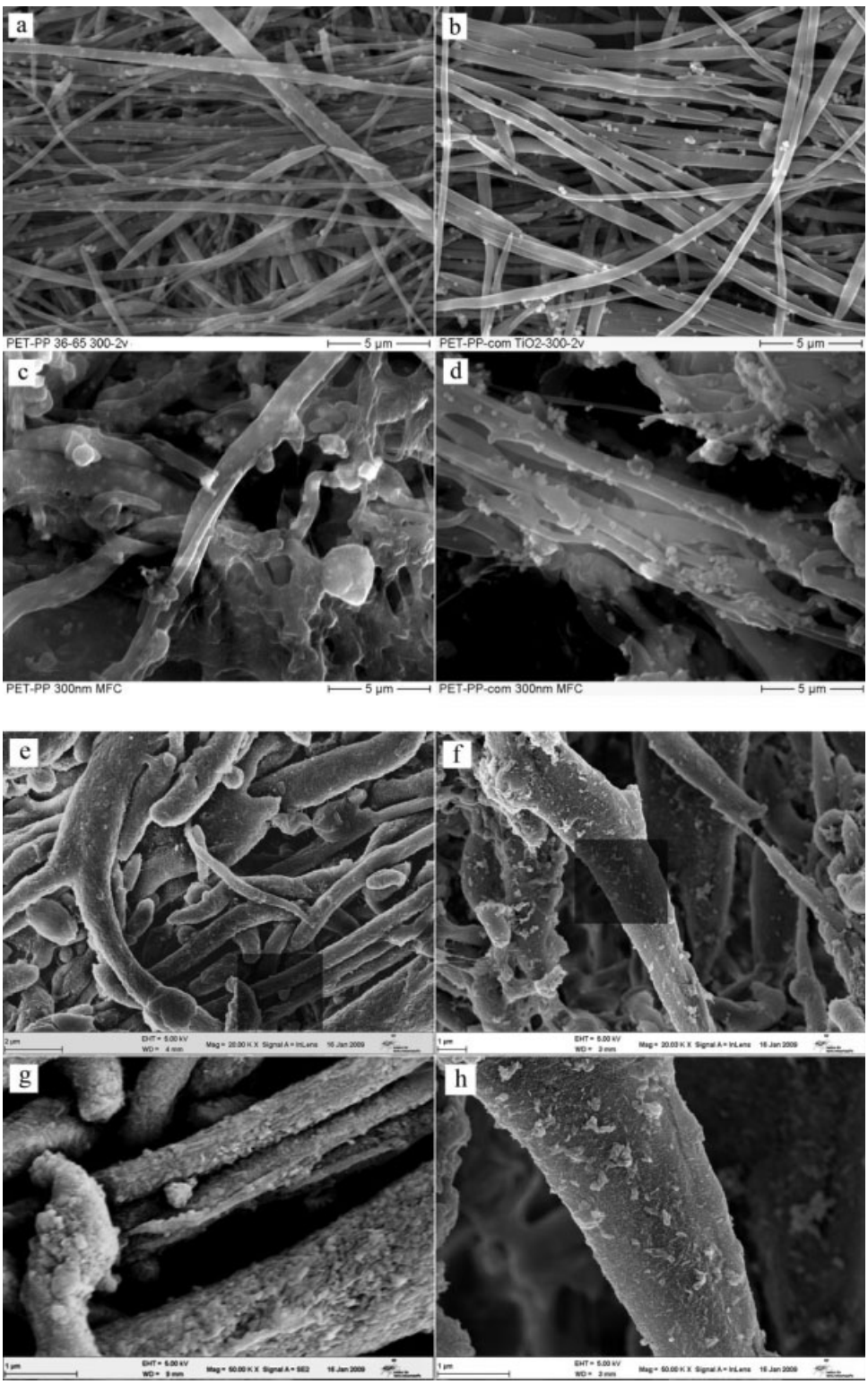

Figure 1 SEM images of PET fibrils in drawn strands and injection-molded specimens (PP is removed by xylene): (a) PET/PP/2T300 drawn strand, (b) PET/PP/C/2T300 drawn strand, (c) PET/PP/2T300 MFC, (d) PET/PP/C/2T300 MFC, (e) PET/PP/2T15 MFC, (f) PET/PP/C/2T15 MFC, (g) high- magnification image of the selected area in (e), and (h) high-magnification image of the selected area in (f).

of their preferential location, the rigid TiO_2 particles act as weak points or stress concentrations. The stress cannot be effectively transferred between the fibrils and matrix when the specimens suffer from sudden impact energy, and the impact strength drops accordingly.[8,6] Similar to the tensile strength

TABLE II
Tensile Properties and Impact Strength of PET/PP and PET/PP/TiO_2 MFC

Specimen	Tensile strength (MPa)	Tensile modulus (MPa)	Impact strength (kJ/m^2)
Neat PP	29.1 ± 1.0	1521.0 ± 58.3	11.1 ± 1.7
PET/PP	30.1 ± 1.7	1995.4 ± 73.0	19.0 ± 2.3
PET/PP/C	31.2 ± 2.0	2190.0 ± 80.5	24.5 ± 4.1
PET/PP/2T300	26.3 ± 2.6	2382.5 ± 97.3	5.6 ± 1.3
PET/PP/C/2T300	29.6 ± 1.6	2311.4 ± 63.8	16.3 ± 1.6
PET/PP/4T300	27.0 ± 0.7	2462.6 ± 71.6	4.0 ± 1.1
PET/PP/C/4T300	30.3 ± 2.0	2318.0 ± 86.9	9.6 ± 2.1
PET/PP/2T15	28.9 ± 2.0	2488.4 ± 100.4	13.2 ± 3.8
PET/PP/C/2T15	30.0 ± 1.7	2406.0 ± 50.6	18.6 ± 1.0

results, the impact strength of the umcompatibilized PET/PP/TiO_2 MFC is much lower compared with the compatibilized PET/PP/TiO_2 MFC. In a composite material, effective energy dissipation is influenced heavily by the interfacial bonding between the matrix and dispersed phase.[34] In the uncompatibilized PET/PP/TiO_2 MFC, the TiO_2 particles are exclusively located in the PET fibrils. As noticed in Figure 2(a), the protruding TiO_2 particles severely damage the PET/PP interface, thus resulting in debonding between the fibrils and matrix. Consequently, the crack easily initiates and propagates through the polymer/fiber interface under impact load, which results in a sharp decrease in impact strength.[35,36] In addition, the damaged PET fibrils also contribute to the droplet of the impact strength. At higher loading of TiO_2 particles (4 vol %) the damage of interface and PET fibrils is more severe, a further decrease in impact strength is thereby observed for the PET/PP/4T300 MFC. In the compatibilized PET/PP/TiO_2 MFC, the TiO_2 particles are dispersed in the PP matrix, the PET fibrils are well preserved. The PET fibril/PP matrix interface is less likely to be damaged because the TiO_2 particles are less prone to protrude out of the isotropic PP. Therefore, higher impact strength of the compatibilized PET/PP/TiO_2 MFC is observed in comparison with the uncompatibilized PET/PP/TiO_2 MFC.

Dynamic mechanical properties

Dynamic mechanical spectra (storage modulus E' and tan δ) as a function of temperature for the PET/PP and PET/PP/TiO_2 MFC are graphically represented in Figure 3. As shown in Figure 3(a), the storage modulus of MFC drops gradually in the whole temperature range. The storage moduli of PET/PP/TiO_2 MFC are very close to one another, these values are noticeably higher than that of the PET/PP MFC. This result is in agreement with the tensile test result but seems to be contradictive to our earlier DMA analysis of the PET/PP/TiO_2 drawn strands: incorporation of TiO_2 particles decreases the E' for all the PET/PP/TiO_2 drawn strands, and the E' drops even more with increasing concentration of TiO_2 particles. Note in the drawn strands both PET and PP phases are well oriented, the decrease in E' for the drawn strands is attributed to the damaged interface (by the TiO_2 particles), which results in poor stress transfer between the fibrils and matrix.[25] In this study, after injection molding the PP phase loses its orientation and forms the continuous phase. The PET fibrils also become much shorter and thicker, some fibril bundles are also noticed [Fig. 2(b)]. Accordingly, the interfacial area between the PET fibrils and PP matrix is greatly decreased. Compared with the PET/PP/TiO_2 drawn strands, the

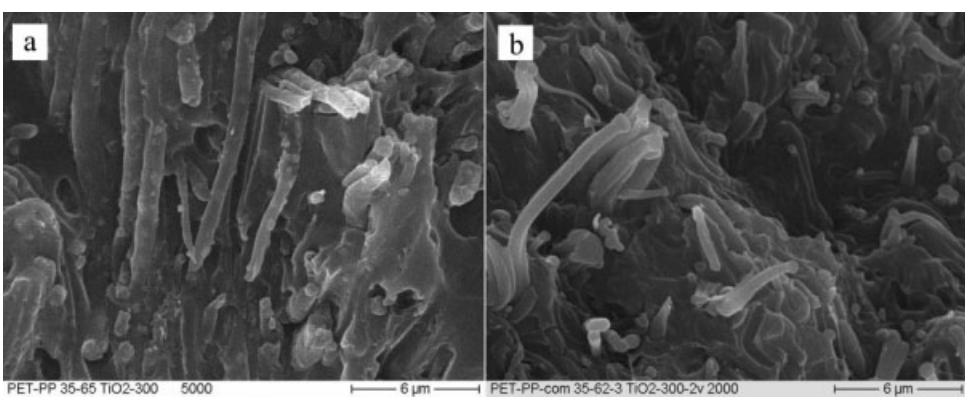

Figure 2 Fracture surfaces of (a) PET/PP/2T300 MFC and (b) PET/PP/C/2T300 MFC.

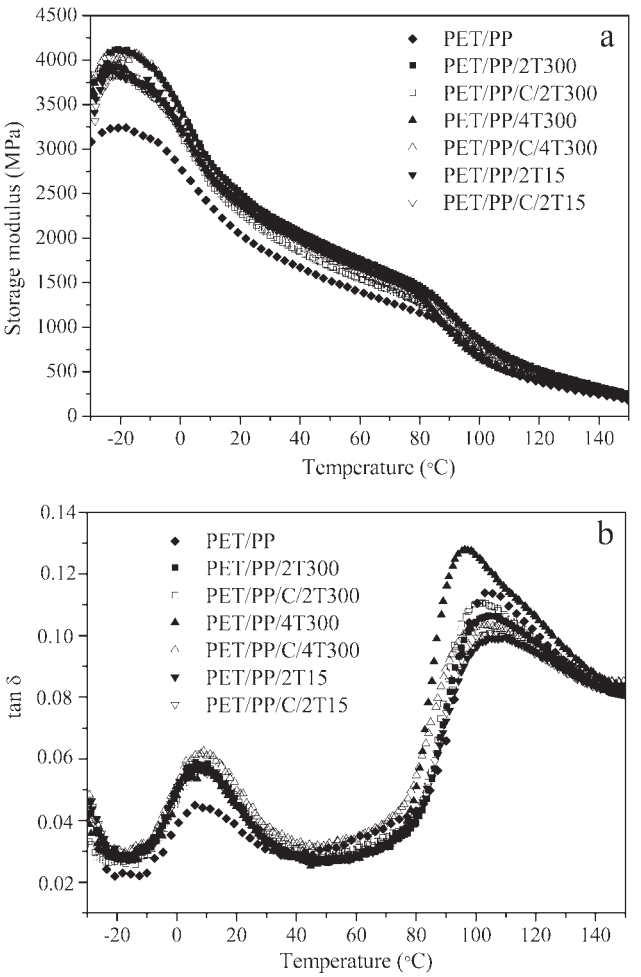

Figure 3 Thermal dynamic curves of the PET/PP and PET/PP/TiO2 MFC: (a) storage modulus vs. temperature and (b) tan δ vs. temperature.

TiO_2 particles in both PET fibrils and PP matrix are less prone to protrude out in the PET/PP/TiO_2 MFC, less interfacial defects are expected. For the PET/PP/TiO_2 MFC the rigid TiO_2 particles contribute to the elevation of storage modulus. Obviously, this positive effect of TiO_2 particles on the storage modulus surpasses the influence of the defects (caused by the TiO_2 particles) at the interface, which decreases the storage modulus.

In the tan δ vs. temperature graph, two relaxation peaks are observed at around 6°C and 103°C, which correspond to the glass transition temperatures (T_g) of PP and PET, respectively.[37,38] The temperature maximum of the relaxation peaks of PP and PET is given in Table III. It is interesting to notice that for the PET/PP/2T300 and PET/PP/4T300 MFC, the maximum of PP relaxation peak appears at the same position as that for the PET/PP MFC (at around 6 °C); whereas for the PET/PP/C/2T300 and PET/PP/C/4T300 MFC, the maximum of PP relaxation peak shifts to a higher temperature (at around 9°C). However, the temperature maximum of PET relaxation peak in the PET/PP/TiO_2 MFC shows the opposite result. The PET relaxation peak in the compatibilized MFC (PET/PP/C/2T300 and PET/PP/C/4T300) reaches its maximum at around 103°C, which is also the temperature maximum of PET relaxation peak for PET/PP MFC. For the PET/PP/2T300 MFC (the uncompatibilized MFC), the tan δ maximum of PET appears at 105.1°C, which is 2°C higher than that of the PET in the PET/PP MFC. However, for the PET/PP/4T300 MFC the tan δ maximum is at around 97°C, which is surprisingly lower compared with other PET/PP/TiO_2 MFC.

The variation of T_g for both PP and PET can be attributed to the preferential location of TiO_2 particles. As shown in Figure 1, for the compatibilized PET/PP/TiO_2 MFC (PET/PP/C/2T300 and PET/PP/C/4T300) where the TiO_2-300 nm particles are preferentially located in the PP matrix, these rigid TiO_2 particles restrict the mobility of the PP chains, thus resulting in the increase of T_g for PP.[11] Similarly, for the PET/PP/2T300 MFC, the preferential location of TiO_2 particles in the PET fibril also leads to an increase of T_g for PET. The noticeable drop of T_g for PET in the PET/PP/4T300 MFC is not unusual. Calcagno et al.[39] investigated the PP/PET/montmorillonite(MMT) nanocomposites in which the MMT clays were preferentially situated in the in the PET phase and in PP/PET interface. The cited author reported that addition of MMT into the blends results in a decrease in T_g of the PET dispersed phase. Similar result was also reported by Feng et al.[40] who observed a decrease in T_g of PA6 in the PP/PA6/MMT composites. Both authors associated this behavior to the presence of the MMT predominantly situated in the PET (or PA6) phase and in the interface that affected the chain mobility. In this study, as discussed before the TiO_2 particles are more prone to protrude out of the PET fibrils at high-TiO_2 loading (4 vol %), resulting increased interactions between PP and PET. Consequently, the T_g of PET in the PET/PP/4T300 MFC shifts to lower temperature.

For the PET/PP/2T15 and PET/PP/C/2T15 MFC, the T_g of PP and PET is not influenced by preferential location of TiO_2-15 nm particles. The tan δ peak

TABLE III
Glass Transition Temperatures (T_g) of PP and PET in PET/PP and PET/PP/TiO_2 MFC

Specimen	T_g of PP (°C)	T_g of PET (°C)
PET/PP	6.1	103.0
PET/PP/2T300	6.3	105.1
PET/PP/C/2T300	9.3	102.2
PET/PP/4T300	6.1	96.7
PET/PP/C/4T300	9.1	103.0
PET/PP/2T15	7.1	105.3
PET/PP/C/2T15	7.2	105.0

of PP for both specimens appears at around 7°C, the maximum of PET relaxation peak is at around 105°C. In both MFC, the TiO_2-15 nm particles are always found in the PET fibrils despite of the difference in concentrations, which contributes to the elevation of T_g for PET.

CONCLUSION

In the injection-molded PET/PP/TiO_2 MFC, the PET fibrils become shorter and thicker compared with those fibrils in the drawn strands. However, the preferential location of TiO_2 particles is preserved: in the uncompatibilized PET/PP/TiO_2 MFC, the TiO_2 particles are dispersed in the PET fibrils; whereas in the compatibilized ones the TiO_2-300 nm particles are preferentially dispersed in the PP phase, the TiO_2-15 nm particles are found in both PET fibrils and PP matrix.

The tensile strength and impact strength of the PET/PP/TiO_2 MFC are lower compared with the PET/PP MFC, because the incorporated TiO_2 particles either damage the PET fibrils or result in defects at the interface. However, an increase in tensile modulus for the PET/PP/TiO_2 MFC is observed, which is in good accordance with the DMA result. The glass transition temperatures of the PP and PET phase in the PET/PP/TiO_2 MFC are greatly influenced by the preferential location of TiO_2 particles: exclusively located in the PP matrix, the T_g of PP in the compatibilized PET/PP/TiO_2 MFC is 3°C higher than that of PP in the uncompatibilized PET/PP/TiO_2 MFC and the PET/PP MFC; for the uncompatibilized PET/PP/TiO_2 MFC the preferential location of TiO_2 particles in the PET fibrils also elevates the T_g of PET.

References

1. Vo, L. T.; Giannelis, E. P. Macromolecules 2007, 40, 8271.
2. Gelfer, M. Y.; Song, H. H.; Liu, L.; Hsiao, B. S.; Chu, B. J Polym Sci Pol Phys 2003, 41, 44.
3. Ginzburg, V. V. Macromolecules 2005, 38, 2362.
4. Feng, J. Y.; Chan, C. M.; Li, J. X. Polym Eng Sci 2003, 43, 1058.
5. Ray, S. S.; Pouliot, S.; Bousmina, M.; Utracki, L. A. Polymer 2004, 45, 8403.
6. Zhang, Q.; Yang, H.; Fu, Q. Polymer 2004, 45, 1913.
7. Ma, C. G.; Mai, Y. L.; Rong, M. Z.; Ruan, W. H.; Zhang, M. Q. Compos Sci Technol 2007, 67, 2997.
8. Li, X.; Park, W.; Lee, J.; Ha, C. Polym Eng Sci 2002, 42, 2156.
9. Chow, W. S.; Mohd. Ishak, Z. A.; Ishiaku, U. S.; Karger-Kocsis, J.; Apostolov, A. A. J Appl Polym Sci 2004, 91, 175.
10. Ray, S. S.; Bandyopadhyay, J.; Bousmina, M. Macromol Mater Eng 2007, 292, 729.
11. Qu, C.; Yang, H.; Liang, D.; Cao, W.; Fu, Q. J Appl Polym Sci 2007, 104, 2288.
12. Filler, N.; Hrnjak-Murgic, Z.; Jelcic, Z.; Kovacevic, V.; Mlinac-Misak, M.; Jasenka, J. Macromol Mater Eng 2002, 287, 684.
13. Champagne, M. F.; Huneault, M. A.; Row, C.; Peyrel, W. Polym Eng Sci 1999, 39, 976.
14. Yoon, K. H.; Lee, H. W.; OK Park, O. Appl Polym Sci 1998, 70, 389.
15. Papadopoulou, C. P.; Kalfoglou, N. K. Polymer 2000, 41, 2543.
16. Heino, M.; Kirjava, J.; Hietaoja, P.; Seppälä, J. J Appl Polym Sci 1997, 65, 241.
17. Xanthos, M.; Young, M. W.; Biesenberger, J. A. Polym Eng Sci 1990, 30, 355.
18. Lepers, J.; Favis, B. D.; Lacroix, C. J Polym Sci Pol Phys 1999, 37, 939.
19. Cheung, M. K.; Chan, D. Polym Int 1997, 43, 281.
20. Pracella, M.; Chionna, D.; Pawlak, A.; surname, A. J Appl Polym Sci 2005, 98, 2201.
21. Li, Z. M.; Yang, M. B.; Xe, B. H.; Feng, J. M.; Huang, R. Polym Eng Sci 2003, 43, 615.
22. Li, Z. M.; Yang, M. B.; Huang, R.; Yang, W.; Feng, J. M. Polyme-Plast Technol 2002, 41, 19.
23. Shen, J. W.; Huang, W. Y.; Zuo, S. W. Macromol Mater Eng 2003, 288, 658.
24. Huang, W. Y.; Shen, J. W.; Chen, X. M.; Chen, H. Y. Polym Int 2003, 52, 1131.
25. Li, W.; Schlarb, A. K.; Evstatiev, M. J Appl Polym Sci, to appear.
26. Evstatiev, M.; Fakirov, S.; Evstatiev, O.; Friedrich, K. Int J Polym Mater 2004, 53, 211.
27. Evstatiev, M.; Fakirov, S. In Polymer Composites: From Nano- to Macro-Scale; Friedrich, K.; Fakirov, S.; Zhang, Z., Eds.; Springer: New York, 2005, Chapter 9, p 149.
28. Evstatiev, M.; Schultz, J. M.; Fakirov, S.; Friedrich, K. Polym Eng Sci 2001, 41, 192.
29. Taepaiboon, P.; Junkasem, J.; Dangtungee, R.; Amornsakchai, T.; Supaphol, P. J Appl Polym Sci 2006, 102, 1173.
30. Friedrich, K.; Evstatiev, M.; Fakirov, S.; Evstatiev, O.; Ishii, M.; Harrass, M. Compos Sci Technol 2005, 65, 107.
31. Li, Z. M.; Yang, W.; Huang, R.; Fang, X. P.; Yang, M. B. Macromol Mater Eng 2004, 289, 426.
32. Jayanarayanan, K.; Thomas, S.; Joseph, K. Compos Part A Appl Sci 2008, 39, 164.
33. Premphet, K.; Horanont, P. J Appl Polym Sci 2000, 76, 1929.
34. Lee, B. S.; Chun, B. C. Polym Compos 2003, 24, 192.
35. Li, Z. M.; Yang, M. B.; Feng, J. M.; Huang, R. J Mater Sci 2001, 36, 2013.
36. Jiang, C.; Zhong, G.; Li, Z. M. Macromol Mater Eng 2007, 292, 362.
37. McCrum, N. G.; Read, B. E.; Williams, G.Anelastic and Dielectric Effects in Polymeric Solids; Wiley: London, 1967.
38. DA Silva, L.; Bretas, R. E. S. Polym Eng Sci 2000, 40, 1414.
39. Calcagno, C. I. W.; Mariani, C. M.; Teixeira, S. R.; Mauler, R. S. Compos Sci Technol 2008, 68, 2193.
40. Feng, M.; Gong, F.; Zhao, C.; Chen, G.; Zhang, S.; Yang, M. Polym Int 2004, 53, 1529.